Automotive Wheel Optimization to Enhance the Fatigue Life

S. Beigzadeh [1], J. Marzbanrad [2*]

[1] *M.Sc. Graduated, School of Automotive Engineering, Iran University of Science and Technology, Tehran, Iran*

[2] *Associate Professor, School of Automotive Engineering, Iran University of Science and Technology, Tehran, Iran*

ARTICLE INFO	ABSTRACT
	Nowadays, lightweight automotive component design, regarding fuel consumption, environmental pollutants and manufacturing costs, is one of the main issues in the automotive societies. In addition, considering safety reasons, the durability of the automotive components, as one of the most important design requirements should be guaranteed. In this paper, a two-step optimization process including topology and shape optimization of an automotive wheel, as one of the most significant chassis components, is studied. At first, topology optimization method with volume and fatigue life constraints is used to obtain the optimal initial lightweight design, followed by shape optimization technique to improve the fatigue life. The results show 31.841% weight and 33.047% compliance reduction by topology and also 652.33% average minimum fatigue life enhancement, by the shape optimization. Therefore, the proposed two-step optimization method is qualified in designing the lightweight automotive wheel. The method used in this study can be a reference for optimization of other mechanical components.

1. Introduction

Automotive lightweight component design is gaining in importance regarding rising environmental demands and ever-tougher emissions standards. In the recent years, several optimization methods were implemented to achieve this goal. Among these methods, topology optimization as a developing structural optimization method, achieved a prominent place in industrial lightweight design process. Topology optimization is an optimization method that modifies the optimum distribution of the material in a given space. This method can be used in the concept stage of design process to obtain the initial lightweight configuration of a product. After that, the inspired design can be optimized by other optimization methods like shape optimization to fulfill the other design requirements. Shape optimization is a structural optimization approach that changes the boundary shapes of the design domain.

Today, the main target of mechanical design is to improve the durability and reliability of a product along with weight reduction [1, 2]. Automotive wheel as one of the vital components of chassis system should fulfill certain requirements (e.g. appropriate weight, stiffness and durability) simultaneously. Since, in-service loadings of automotive wheel are cyclic in nature, therefore the fatigue characteristics of the wheel must be considered in the design process [3].

Here are some previous studies about the optimization of mechanical components regarding the fatigue characteristics: Haiba et al. [4] introduced a new optimization algorithm based on eliminating the parts of structure with the maximum fatigue life representing unnecessary use of material with an optimization constraint to prevent the reduction of fatigue life under the initial design level. Desmorat et al. [5] implemented topology optimization in damage governed low cycle

*Corresponding Author
Email Address: *marzban@iust.ac.ir*

fatigue in order to maximize fatigue life by optimizing the shape of a structure in cyclic plasticity combined with Lemaitre damage law. Topac et al. [6] applied finite element analysis to analyze the fatigue life performance of a vehicle wheel subjected to radial loading. The local changes to the wheel disc were made to improve the fatigue life of the wheel. Wan Muhamad et al. [7] used the shape optimization method with fatigue constraint for weight reduction of an automotive rear spindle. Erik Holmberg et al. [8] introduced topology optimization method with high-cycle fatigue-constraints and provided some typical analysis examples by this method. Seung Hyun Jeong et al. [9] expressed the significance of regarding fatigue failure in the innovative designs of topology optimization method and contributed to a new dynamic fatigue-constrained topology optimization method. The other recent contributions to topology optimization considering fatigue life as an important design factor are [10] and [11]. In this research, a design process is devised based on topology and shape optimization methods regarding the durability of the automotive wheel and is briefly introduced through following section.

2. Design Process Scheme

In this research, the automotive wheel design process includes three stages. The first stage is the data acquisition of the automotive in-service loadings. Since, the input data for fatigue analysis are the time-variant mechanical loadings, which are introduced to the automotive wheel through the ride, some virtual proving ground tests are done through multi-body dynamic analysis software, *Adams/car*, and the most severe load-time histories resulted from the tests are identified. The output result of stage I is used further in stage II. The flowchart of the first stage is given in Figure 1.
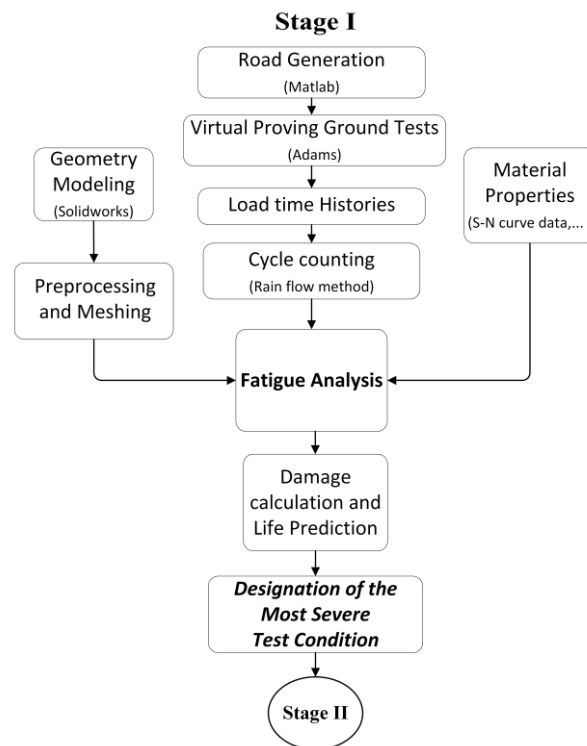

Figure 1: Flowchart for stage I

By the knowledge of automotive wheel in service loadings, the design process can be continued by a two-step optimization process including topology and shape optimization. Structural optimization is being implemented and developed through some finite element analysis software for practical problems. In this study, a commercial FEA software, Hyperworks *(Optistruct)* is employed for topology and shape optimization. It should be noted that, in optimization problems with fatigue constraint, Hyperworks solver, *Radioss* calculates the fatigue life in all iterations of solving procedure to control the fatigue constraint satisfaction.

At the first stage of the optimization, topology optimization method is used to maximize the stiffness, as one of the most important automotive wheel design requirements. By using this approach, the initial lightweight design of the wheel is obtained.The flowchart of the second stage is given in Figure 2. At the next stage, shape optimization method with fatigue

constraint is applied to ensure the durability of the initial design that leads to fatigue life enhancement.

In this stage, two cases (A and B) are considered for shape optimization. The distinction of two cases is specified by the different regions of the wheel that are considered for the optimization.

In the end of the optimization process, these cases are compared to each other in order to achieve the final design of the wheel.The flowchart of the third stage is given in Figure 3.
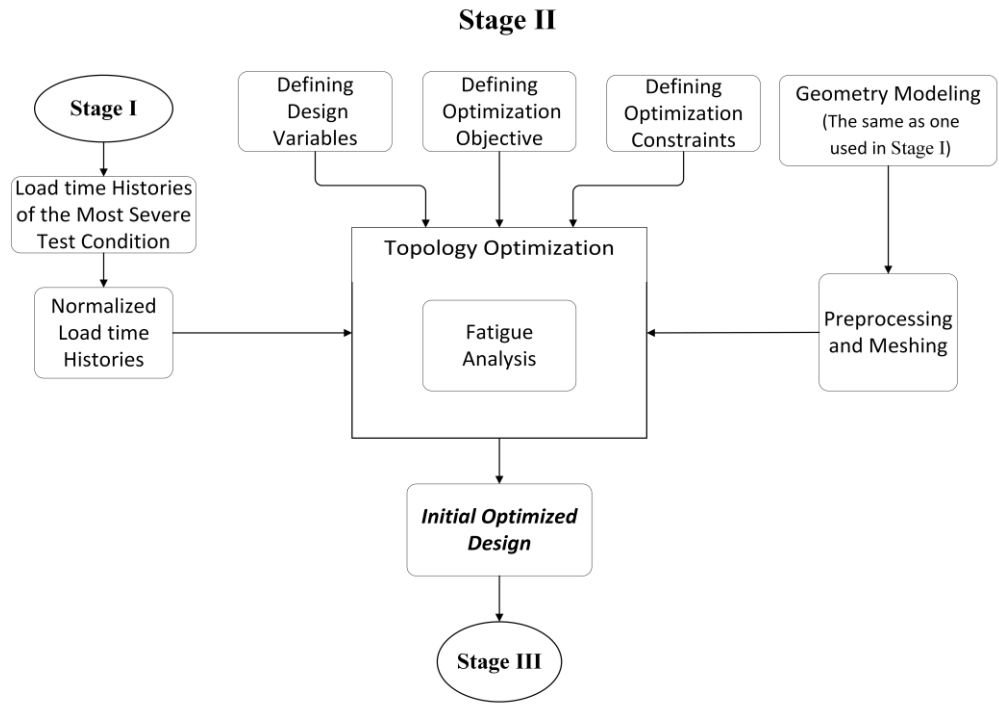
Stage II

Figure 2: Flowchart for Stage II
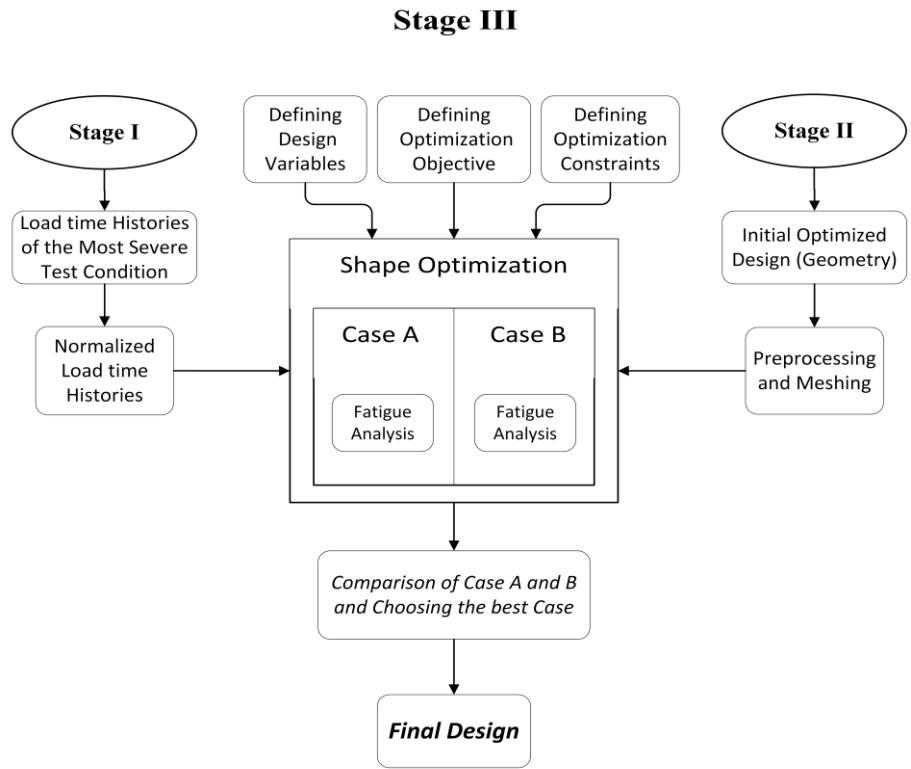
Stage III

Figure 3: Flowchart for Stage III

3. Stage I

The main purpose of stage I is recognizing the automotive wheel loadings. The knowledge of mechanical in-service loadings of components is the first step of durability design and optimization. Automotive wheels are the intermediate parts between road surface and the vehicle. In the normal driving conditions and unintended events (braking conditions, driving over road bumps), the mechanical loadings, exerted upon the wheels are variable and multi-axial [12].

In this section, some virtual proving ground tests are considered to recognize the critical load-time histories, introduced to automotive wheel. The first stage of these simulation tests is generation of some standard roads as discussed in the following subsection.

3.1 Road Generation

Road roughness classification based on the power spectral density has been proposed by the International Organization for Standardization (ISO). The road surface roughness is expressed as Power spectral density (PSD). The relationship between the road surface PSD and spatial frequency, φ can be approximated as (1) [13],

$$G_u(\varphi) = C_{sp} * \varphi^{-N} \tag{1}$$

Where, $G_u(\varphi)$ is the power spectral density of the elevations of road surface profile and C_{sp}, and N are constants. Fitting the expression to the curves obtained by measured data produces the values of C_{sp} and N as given in Table 1 [13].

Table 1: Constant values of C_{sp} and N [13]

Type	Road Profile	N	C_{sp}
A	Smooth Runway	3.8	4.3×10^{-11}
B	Smooth Highway	2.1	4.8×10^{-7}
C	Ride and Handling Track Can-Can	1.8	2.27×10^{-6}
D	Highway with gravel	2.1	4.4×10^{-6}
F	Fatigue Track Can-Can	2.9	3.42×10^{-5}
G	Pasture	1.6	3×10^{-4}

The method explained by Hullender [14] is used to create some rough road surfaces. In this study, the road profiles, types B, C and D, are generated by Matlab code. These roads are used further in virtual proving ground tests, subsection 3.2. The surface elevations of generated roads are shown in Figures 4, 5 and 6.
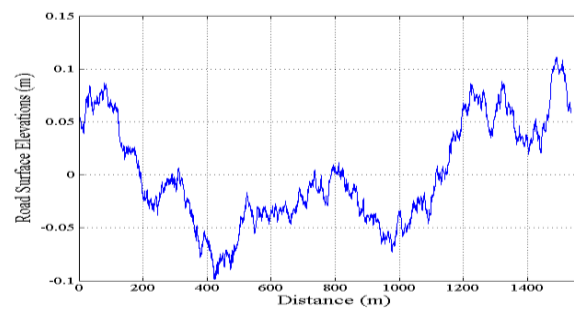

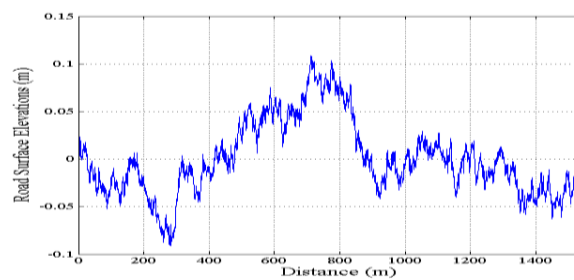**Figure 4:** Road type B surface elevations

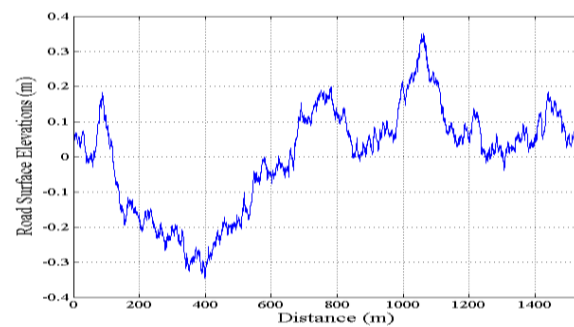**Figure 5:** Road type C surface elevations

Figure 6: Road type D surface elevations

3.2 Virtual Proving Ground Tests

The virtual proving ground is an approach for simulation of the road and automotive model and the related systems such as powertrain, suspension, steering system and etc. Through the development of this approach, the vehicle performance can be analyzed through various virtual tests [15]. The road type, a vehicle is driven on, speed and type of driving, affects the design life. Therefore,

performing different road test simulations is essential to consider these effects.

In this study, Adams/car software is used for simulation of some virtual proving ground tests to obtain the load-time histories of normal, lateral and longitudinal forces that exert upon automotive wheel during the ride. The tests No.1 to 9 are listed with their specifications in Table 2.

Table 2: Virtual proving ground tests

Test No.	Test Type	Road Type	Initial Velocity (Km/h)
1	Straight-Line Constant Velocity	B	100
2	Straight-Line Constant Velocity	C	75
3	Straight-Line Constant Velocity	D	50
4	Straight-Line Braking	B	100
5	Straight-Line Braking	C	75
6	Straight-Line Braking	D	50
7	Constant Radius Cornering	C	30
8	Constant Radius Cornering	C	40
9	Constant Radius Cornering	C	50

The roads, generated by Matlab code, are imported to Adams/car and visualized by the Road Builder module. So, the road types A, B and C are recalled for road test simulations. Also, the Ferrari Testarossa car model is recalled from the Adams/car library. By the roads and the car model at the hand, the full-vehicle analysis is applied to simulate the road tests, including: a) Maintain straight test maneuver, b) Braking test maneuver and c) Constant Radius cornering maneuver.

The tests No 1, 2 and 3 are done by Maintain straight test maneuver, so the steering input is remained straight and the velocity is maintained constant. The tests No 4, 5 and 6 are done by Braking test maneuver, so the steering input is remained straight and the initial velocity is decreased gradually by braking. The tests No.7, 8 and 9 are done by Constant radius cornering maneuver, so the car turns around a constant radius route (30 meters). By the road test simulations the required load time histories are available. Some sample load-time histories resulted from the simulated tests are presented in Figures 7, 8 and 9.
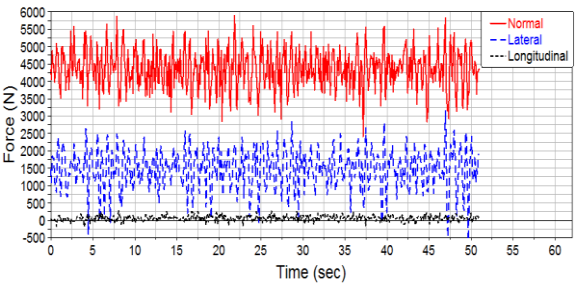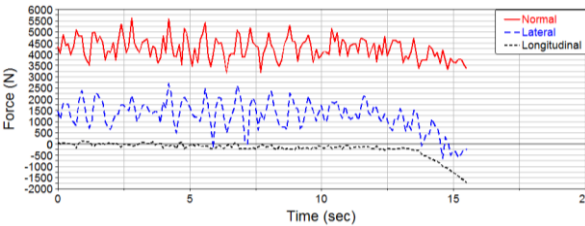

Figure 7: Test No. 3 - Load time histories

Figure 8: Test No. 6 - Load time histories
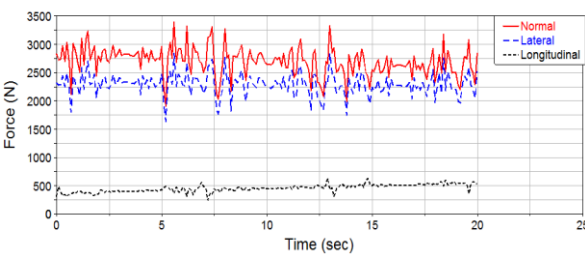
Figure 9: Test No. 9 - Load time histories

The primary design of automotive wheel is modeled, firstly. Then, the fatigue analysis is studied to identify the most severe test condition and corresponding load-time histories. These load-time histories are the representative of the variable amplitude loadings that a typical automotive wheel, encounters and might lead to nucleation of microscopic cracks, growth of the cracks and fracture.

3.3 Geometry, Meshing and Material

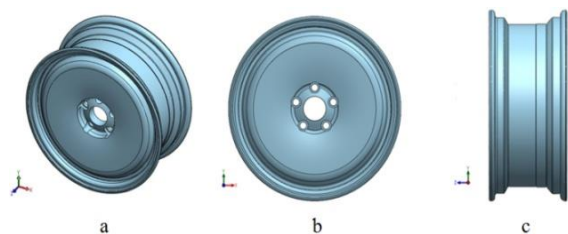The geometrical model of the primary automotive wheel is represented in Figure 10.

Figure 10: a) Trimetric, b) front and c) side views of the wheel

Typical wheel size of 7.5j*18" is considered (7.5, is inner width of wheel in inches, symbol j, indicates the shape of the wheel on the place where the tire bead sits on the wheel and 18, is nominal wheel diameter in inches). The finite element model for automotive wheel is shown in Figure 11.
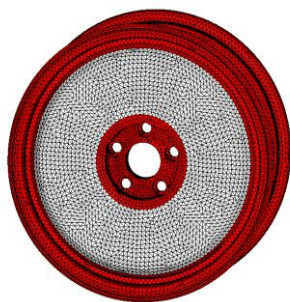

Figure 11: Automotive wheel finite element model

Aluminum alloy, AlSi7Mg0.3 known as A356, is considered as the standard material in manufacturing of the automotive wheel. This alloy has a wide field of applications in the automotive and airplane industries because of good cast ability, machining, welding and corrosion resistance characteristics. The properties of A356 aluminum alloy are given in Table 3.

Table 3: A356 aluminum alloy properties

Alloy Type	AlSi7Mg0.3 (A356)
Manufacturing method	Mold Casting
Heat treatment	T6
Tensile Strength, Yield	152 MPa
Tensile Strength, Ultimate	228 Mpa
Elongation at Break	≥ 0.03
Modulus of Elasticity	72.4 Mpa
Poisson ratio	0.33
Density	$2670 \frac{kg}{m^3}$

3.4 Fatigue Analysis

The three aspects to the fatigue analysis definition are fatigue material properties, fatigue parameters and fatigue loadings definitions.

3.4.1 Fatigue Material Properties

The fatigue material properties are obtained from the material curve S-N curve shown in Figure 12. The material S-N curve should be modified to account for all the factors such as surface finish and manufacturing method.
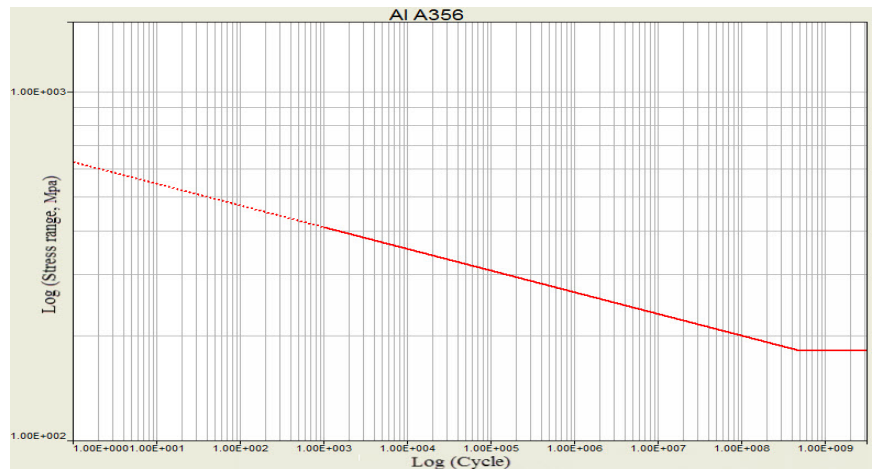

Figure 12: Stress-Life curve of A356

3.4.2 Fatigue Parameters

The fatigue parameters are defined by the knowledge of cycle counting method, mean stress correction and stress combination method. Since, the automotive wheel loadings are time-variant; a cycle counting method should be used to break the variable amplitude load-time histories to simple constant amplitude load cycles. For this reason, Rain flow as the most popular cycle counting approach is used. Also, the automotive wheel fatigue is categorized as a high cycle one, so the mean stresses, affects the fatigue behavior remarkably. So the known Gerber criterion is used for mean stress corrections. Furthermore, considering the multi-axial nature of the stress, an approach should be used to reduce the multi-axial stress state to an equivalent uniaxial stress state. For this purpose, Signed Von Misses approach is used to obtain the equivalent stress as the input data of stress-life theory to calculate the fatigue life.

It should be noted that a fatigue strength reduction factor have to be taken into account to adopt the S-N curve for a real-life model., therefore a fatigue strength reduction factor of 1.1 is considered for this purpose. All the fatigue parameters definitions are set up according to Table 4.

Table 4: Fatigue parameters definition

Analysis Type	Stress - Life (S-N)
Stress Combination method	Signed Von Mises
Mean Stress Combination	Gerber method
Cycle Counting Method	Rain-Flow
Surface Finish Factor	0.95
Fatigue Strength Reduction Factor	1.1

3.4.3 Fatigue Loadings

Fatigue loadings are defined through attribution of static analyses to the load time histories. When there are several loadings that vary independently from each other and act simultaneously, the principle of linear superposition can be used to combine all the loadings together to determine total stress at each calculation node. The quasi-static superposition is denoted by (2) [7]:

$$\sigma(x^K, t) = \sum_{K=1}^{n_S} \sigma_K^{(x^k)} \frac{L_K(t)}{L_K^0} \qquad (2)$$

Where,

$\sigma(x^k, t)$ is the total stress tensor for every node,

$L_K(t)$ is the time variation of the kth load time history

$\sigma_K^{(x^k)}$ and L_K^0 is the kth stress tensor and load magnitude from static analysis

x represents each nodal position.

k is the counter of unit load cases to the upper limit (n_s)

By the calculation of the total stress at each node, and using S-N theory, the fatigue life can be estimated through the Palmgren-Miner damage rule. By the Rain flow method, the different load levels and the corresponding number of repetition of each load level (n_i) are designated.

According to Palmgren-Miner rule if there exists different stress levels and the average number of cycles to failure at the ith stress amplitude, is N_i then the damage of component in each nodal position, $D(x)$ is calculated by (3) [16]:

$$D(x) = \sum_{i=1}^{m} \frac{n_i(x)}{N_i(x)} \qquad (3)$$

It should be noted that, each n_i can be expressed by a fraction of total life, n. Therefore, the total life can be calculated by equating (3) to the number 1 [16].

The fatigue loadings are set up for each test (Table 2) according to corresponding resultant load-time histories. The loadings and boundary conditions are presented in Figures 13 and 14, respectively. The boundary conditions are set, so that the wheel displacements are fixed at the wheel bolt mounting locations in all degrees of freedom.

Fatigue analysis is done with load-time histories resulted from tests No. 1 to 9 to identify the most severe test condition.
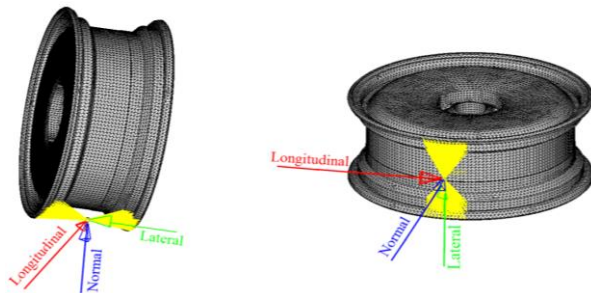
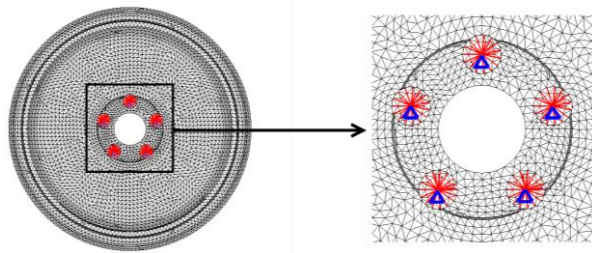**Figure 13:** Normal, lateral and longitudinal loadings

Figure 14: Boundary conditions

The results of fatigue analysis are shown in Table 5. By comparison of fatigue life cycles corresponding to each driving test, it is clear that the automotive wheel under the test No. 3 has the lowest life. Therefore, the test No.3 is the representative of the most severe test condition.

Table 5: Fatigue analysis results (Tests No. 1 to 9)

Test (No.)	Fatigue Life (Cycles)
1	$8.295*10^{18}$
2	$5.320*10^{14}$
3	$2.561*10^{12}$
4	$4.509*10^{12}$
5	$2.965*10^{13}$
6	$1.030*10^{13}$
7	$5.031*10^{19}$
8	$6.922*10^{15}$
9	$7.601*10^{19}$

The fatigue life contour of automotive wheel, related to test No. 3, is shown in Figure 15.
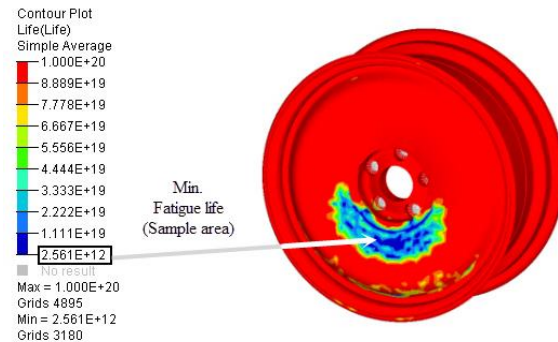

Figure 15: Fatigue life contour - Test No. 3

4. Stage II

The main purpose of stage II is obtaining the initial optimized design through topology optimization method. There are several methods to formulate topology optimization problems; including: Homogenization method [17], Bi-directional Evolutionary Structural Optimization (BESO) [18] and Solid Isotropic Microstructure with Penalization (SIMP). SIMP method is presently the most common FE-based topology optimization approach. *Optistruct*, applies SIMP method for topology [19] and Perturbation Vector Approach for shape optimization formulation [20].

4.1 Topology Optimization

4.1.1 Topology Optimization Theories

Topology optimization based on SIMP method is a mathematical technique that optimize the material distribution for a structure within a given package space. Using this method, the design domain is discretisized to finite elements. The fictionous density of material, x_e is assumed to be the design variable $(0 \leq x_e \leq 1)$. The relationship between initial element density, ρ and the optimized density, ρ_0 is presented by (4) [19, 21],

$$\rho = x_e \, \rho_0 \qquad (4)$$

The topology optimization problem is generally defined to minimize the compliance of structures under a volume constraint. In the SIMP method (density method with the penalization of

intermediate densities), an artificial isotropic material is presented and material density variables are used to interpretation of the structural configuration.

To achieve penalized intermediate densities, the formulation between Young's modulus, E, Young's modulus of the fully solid material, E_0 and the penalty factor, p is presented by (5) [21],

$$E = (x_e)^p E_0 \qquad (5)$$

Where $p > 1$.

Similarly, the equation between the initial stiffness matrices of element, k_0 and optimized stiffness matrix for solid material, k is expressed by (6) [21],

$$k = (x_e)^p k_0 \qquad (6)$$

By considering the mentioned assumptions the topology optimization problem can be formulated as (7) [21],

$$min \ C(x_e) = F^T U = U^T K U = \sum_{e=1}^{n} u_e^T K u_e = \sum_{e=1}^{n} (x_e)^p u_e^T k_0 u_e, \qquad (7a)$$

$$s.t. \quad F = KU, \ \int_\Omega \rho \, d\Omega - M_0 \le 0 \qquad (7b)$$

$$0 < x_{min} \le x_e \le x_{max} \le 1 \qquad (7c)$$

Where, C is compliance of the structure, U and K are the vector of displacement and global stiffness matrix, respectively. Also, u_e is the element nodal displacement vector, F is the force vector, and n is the total number of elements. The total mass of the structure must be less than quantity denoted by M_0, [19, 21]. The optimization problem, stated as (7), can be solved iteratively by numerical optimization methods. *Optistruct*, uses an iterative local approximation method to solve optimization problems. The general form of (7) can be stated as (8) [22]:

$$min. \quad h_0(x) \qquad (8a)$$

$$s.t. \quad h_i(x) \le \hat{h}_i(x), \quad for \ i = 1, \dots, m \qquad (8b)$$

$$\underline{x}_j \le x_j \le \underline{x}_j \qquad , \quad for \ j = 1, \dots, n \qquad (8c)$$

The iterative method initializes by assigning an initial value to the design variables. The procedure is continued by evaluation of the cost and constraint function and their sensitivities in order to modify the design variables through an optimization algorithm. The optimization algorithm, searches the design space iteratively for the new design variables that decreases (or increases) the objective function value while satisfying the constraints. The iterative optimization procedure using approximation techniques is introduced through a flowchart shown in Figure 16.

Figure 16: The iterative optimization procedure using approximation techniques [22]

Since, the cost and constraint functions should be computed numerically by a finite element analysis and also the multiplicity of design variables, the repeated analyses are computational cost. Therefore, to deal with such large scale problems, the approximation methods are developed to break the primary optimization problem to a sequence of sub problems that can be conveniently solved by a dual formulation.

The method of moving asymptotes (MMA) [23] and its mother method, convex linearization method (CONLIN) [24] are the extension to the approximation concepts approach. These methods substitute the primary optimization problem with explicit sub problems that are convex and separable. In other words, then-dimensional problem is changed to n one-dimensional

problems, which make the functions and their computations simpler. The general formulation of the MMA is briefly described below:

Consider the iteration point x^k limited by the upper and lower values of $L_j^{(k)}$ and $U_j^{(k)}$ (9) [23],

$$L_j^{(k)} < x_j^{(k)} < U_j^{(k)} \tag{9}$$

Then the approximation $\tilde{h}_i^{(k)}(x)$ of the arbitrary function $h_i^{(k)}(x)$ can expressed as (10) [23]:

$$\tilde{h}_i^{(k)}(x) = r_i^{(k)} + \sum_{j=1}^{n}\left(\frac{p_{ij}^{(k)}}{U_j^{(k)}-x_j} + \frac{q_{ij}^{(k)}}{x_j-L_j^{(k)}}\right) \tag{10}$$

Where functions $p_{ij}^{(k)}$, $q_{ij}^{(k)}$ and $r_i^{(k)}$ are:

$$p_{ij}^{(k)} = \begin{cases} (U_j^{(k)} - x_j^{(k)})^2 \dfrac{\partial h_i}{\partial x_j}, & if\ \dfrac{\partial h_i}{\partial x_j} > 0 \\ 0, & if\ \dfrac{\partial h_i}{\partial x_j} \leq 0 \end{cases}$$

$$q_{ij}^{(k)} = \begin{cases} 0, & if\ \dfrac{\partial h_i}{\partial x_j} \geq 0 \\ -\left(x_j^{(k)} - L_j^{(k)}\right)^2 \dfrac{\partial h_i}{\partial x_j}, & if\ \dfrac{\partial h_i}{\partial x_j} < 0 \end{cases}$$

$$r_i^{(k)} = h_i\left(x^{(k)}\right) - \sum_{j=1}^{n}\left(\frac{p_{ij}^{(k)}}{U_j^{(k)} - x_j^{(k)}} + \frac{q_{ij}^{(k)}}{x_j^{(k)} - L_j^{(k)}}\right)$$

By calculating the derivatives of the function $h_i^{(k)}(x)$, and choosing the proper values of $L_j^{(k)}$ and $U_j^{(k)}$, the optimization problem described in (8) is substituted by the sub problem given in (11) [23].

$$min. \quad \sum_{j=1}^{n}\left(\frac{p_{0j}^{(k)}}{U_j^{(k)}-x_j} + \frac{q_{0j}^{(k)}}{x_j-L_j^{(k)}}\right) + r_0^k \tag{11a}$$

$$\sum_{j=1}^{n}\left(\frac{p_{ij}^{(k)}}{U_j^{(k)}-x_j} + \frac{q_{ij}^{(k)}}{x_j-L_j^{(k)}}\right) + r_0^k \leq \hat{h}_i,\ for\ i = 1, \dots, m \tag{11b}$$

$$\max\left\{\underline{x}_j, \alpha_j^{(k)}\right\} \leq x_j \leq \min\left\{\overline{x}_j, \beta_j^{(k)}\right\} \quad for\ j = 1, \dots, n \tag{11c}$$

The $\alpha_j^{(k)}$ and $\beta_j^{(k)}$ are called move limits and should be chosen so that, $L_j^{(k)} < \alpha_j^{(k)} < x_j^{(k)} < \beta_j^{(k)} < U_j^{(k)}$

As mentioned before, the subproblems generated by CONLIN or MMA method that have the properties of convexity and separability can be solved by dual method formulation. In dual formulation, the constrained primal minimization problem is changed to maximizing a dual function in dual space of Lagrange multipliers that are associated with active constraints. Since, the optimization is performed in dual space that has relatively low dimension depending on the number of active constraints; this method can handle the problems with immense design space. *Optistruct*, employs the dual method for topology optimization and that's due the large number of design variables with limited much fewer constraints. The principles of dual formulation can be found in [25].

4.1.2 Topology Optimization Set-Up

Topology optimization method with volume and fatigue constraints is implemented for stiffness maximization, as one of the most automotive wheel requirements, to obtain the initial lightweight design. The optimization is done by Hyperworks solver, *Optistruct* using dual formulation. The topology optimization problem is set up by determination of design variable (design domain), objective function and optimization constraints according to Table 6.

Table 6: Topology optimization definitions

Objective Function	*Minimize weighted Compliance* (*Maximize Stiffness*)
Optimization Constraints	*Volume Fraction Constraint* (*Upper bound constraint of 20% for the designable volume*)
	Fatigue Life Constraint (*Lower bound constraint for Min. fatigue life = $5*10^8$ cycles of loading*)
	Manufacturing constraint (*Cyclical symmetry*)

It should be noted that sometimes the design concepts resulted from topology optimization are not manufacturable. For this reason, *Optistruct* embedded

several manufacturing constraints to ensure the manufacturability of the designs. Since, the automotive wheel is axisymmetric, a pattern grouping constraint named cyclical symmetry is also considered. By cyclical symmetry, the design is repeated around a central axis. In optimization problems with fatigue constraint, Hyperworks solver, *Radioss* calculates the fatigue life at all iterations of solving procedure to control the fatigue constraint satisfaction. Therefore,

the load-time histories resulted from the most critical test condition, Test No. 3, are used in fatigue analysis. These load-time histories are normalized by the maximum magnitude of each load (Table 7), corresponding to each load-time history. The normalized load-time histories are shown in Figures 17, 18 and 19. The loading and boundary conditions for topology optimization is the same as shown in Figures 13 and 14.

Table 7: Max. Magnitude of loads - Test No.3

Load Type	Max. Magnitude of the Load
Normal	5906.541 N
Lateral	3151.067 N
Longitudinal	275.027 N
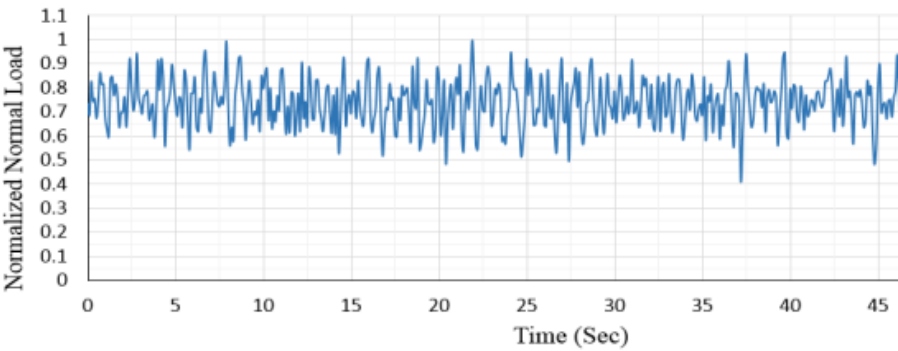
Figure 17: Normalized Normal load-time history - Test No. 3
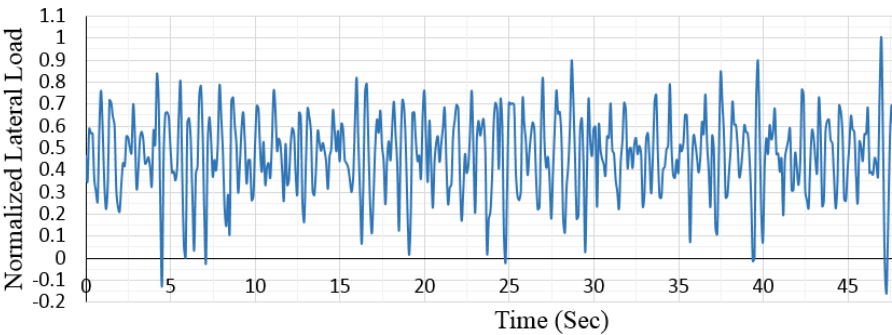
Figure 18: Normalized Lateral load-time history - Test No. 3
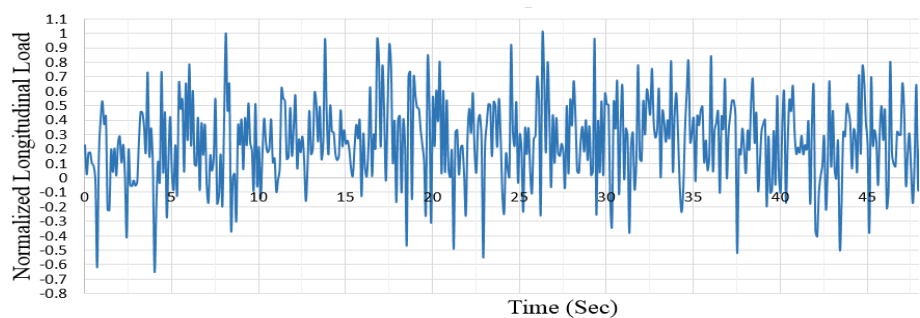
Figure 19: Normalized Longitudinal load-time history -Test No. 3

4.2 Topology Results

The solving procedure of topology optimization problem by *Optistruct* is ended after 31 iterations. The optimized design after topology optimization is presented in Figure 20. The weight and the weighted compliance of the wheel after topology optimization is reduced 31.841% (Table 8) and 33.047 % (Figure 21), respectively. Figure 21 shows the variations of the objective function through the topology optimization process. The fatigue life constraint is satisfied with min. fatigue life of 4.798 $*10^{10}$ at the last iteration (Figure 22).

Figure 20: The optimized design after topology optimization

Table 8: Mass reduction after topology optimization

Initial Mass	Final Mass	Reduction
16.1977 Kg	11.0401 Kg	31.841%
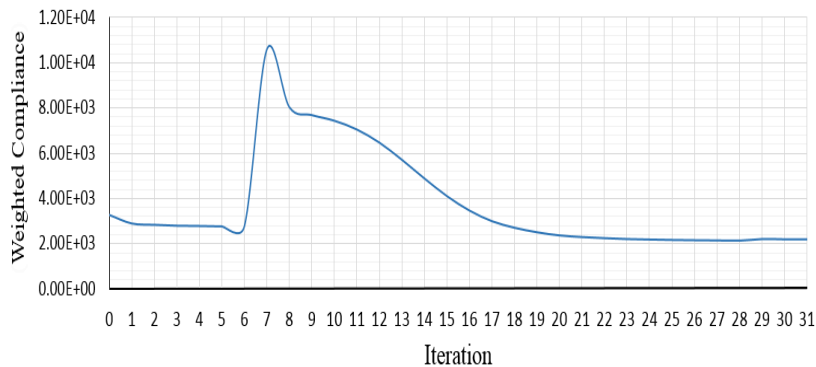
Figure 21: Objective function versus solving iteration
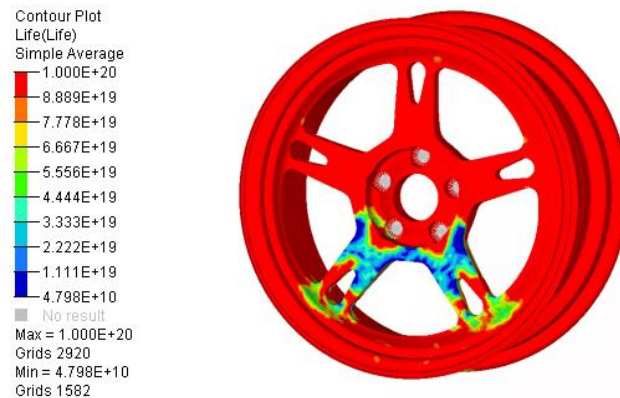
Figure 22: Fatigue life contour at last iteration of topology optimization

5. Stage III

By topology optimization, the initial design of the wheel is obtained. In this stage, shape optimization method with fatigue constraint is applied to the automotive wheel to ensure the durability of the optimized design that leads to fatigue life enhancement.

5.1 Shape Optimization Theories

Shape optimization based on perturbation vector approach is a way of defining shape changes to finite element model without changing the topology of structures. In this approach, shapes are defined by summation of vector of nodal coordinates, x_0 that represents the initial configure of the structure before optimization and perturbations, μ , as (12) [20].

$$x = x_0 + \mu \tag{12}$$

The optimized shape of structure x can be obtained with a linear combination of the weighted perturbations and element nodal coordinates presenting basis shapes, as (13) [20].

$$x = x_0 + \sum_{i=1}^{k} \omega_i \mu_i \tag{13}$$

Where, k is the number of shapes and ω is the weight of perturbations.
The purpose of shape optimization is to find the best weights that define the optimal shape [20].

Optistruct uses a primal feasible direction method for the optimization problems with a limited number of design variables. The feasible direction method is explained in detail in [26, 27]. This primal method searches for the optimum design through the original design space, in contrast to dual method that handles the problem in dual space. The choice of optimizer (primal or dual) is made automatically by *Optistruct* that depends mainly on the number of the design variables.

5.2 Shape Optimization Set-Up

The optimized topology of the wheel is retrieved for shape optimization. Since the geometry of optimized wheel by topology optimization method is more complex than the primary model, re-meshing of the retrieved model is necessary. Meshing with smaller element size leads to better adaption of mesh on the curvatures of model surfaces and more accurate results. The re-meshed model is shown in Figure 23.

Figure 23: Re-meshed model of wheel

Free-shape optimization method is selected for this phase of optimization. Free-shape is an automated way to modify the structure shape based on the set of nodes that can move totally free on the boundary to find the optimal shape. The optimization problem is set up by determination of design variable, objective function and optimization constraints according to Table 9.

In this stage, two different cases are considered for shape optimization problem in order to compare and study the effect of shape changes in each case, on fatigue life. The differences between the two cases, called A and B, are the distinct selection of nodes, as design variables. The coordinates of the selected nodes are the design variables of optimization problem.

The cases A and B are presented in Figure 24 and Figure 25, respectively. The loadings and boundary conditions are the same as which, considered for topology optimization.
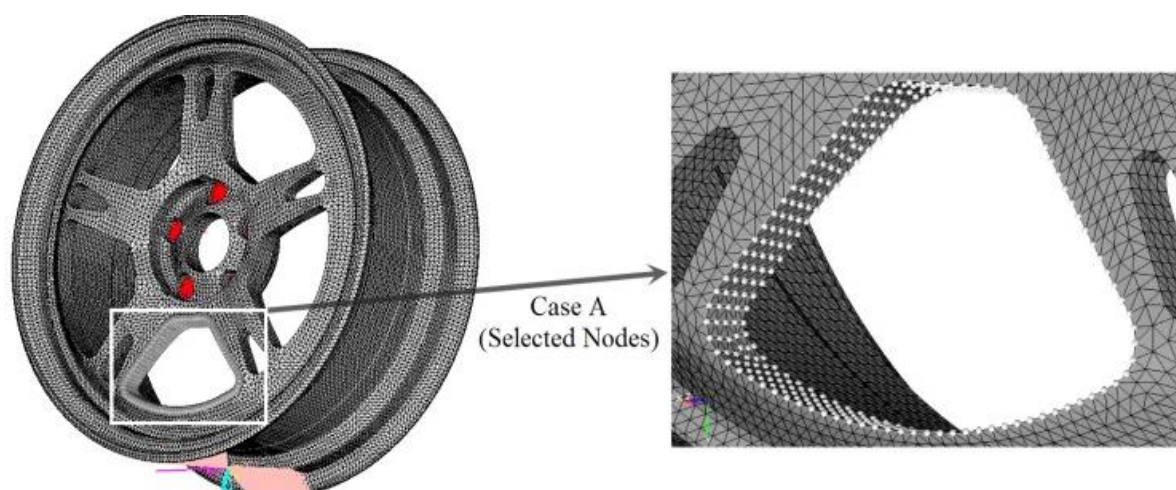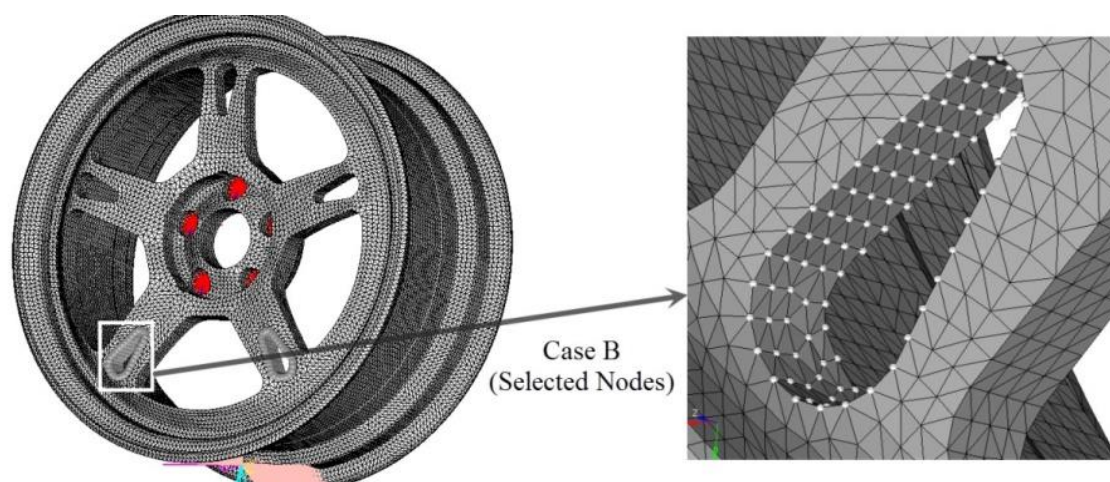
Table 9: Shape optimization definition

Objective Function	Minimize Volume
Optimization Constraints	Fatigue Life Constraint (Lower bound constraint for Minimum fatigue life = $1*10^9$ cycle of loading)

Figure 24: Free-shape optimization - Case A

Figure 25: Free-shape optimization - Case B

Automotive Wheel Optimization to Enhance the Fatigue Life

5.3 Shape Results

The results of shape optimization, Case A, show 0.75% volume reduction as objective function and average minimum fatigue life enhancement about 652.33%.

The results for Case B are 0.01% and 10.843%, respectively (Table 10).

Table 10: Fatigue life results of shape optimization

	Average Minimum Fatigue life Results (cycles)		
	Top 0.1%	Top 1%	Top 5%
Before Optimization	$2.982*10^{10}$	$2.982*10^{11}$	$1.490*10^{12}$
After Optimization (Case A)	$2.245*10^{11}$	$2.244*10^{12}$	$1.122*10^{13}$
After Optimization (Case B)	$3.305*10^{10}$	$3.305*10^{11}$	$1.652*10^{12}$
Enhancement (Case A)	652%	652%	653%
Enhancement (Case B)	10.83%	10.83%	10.87%
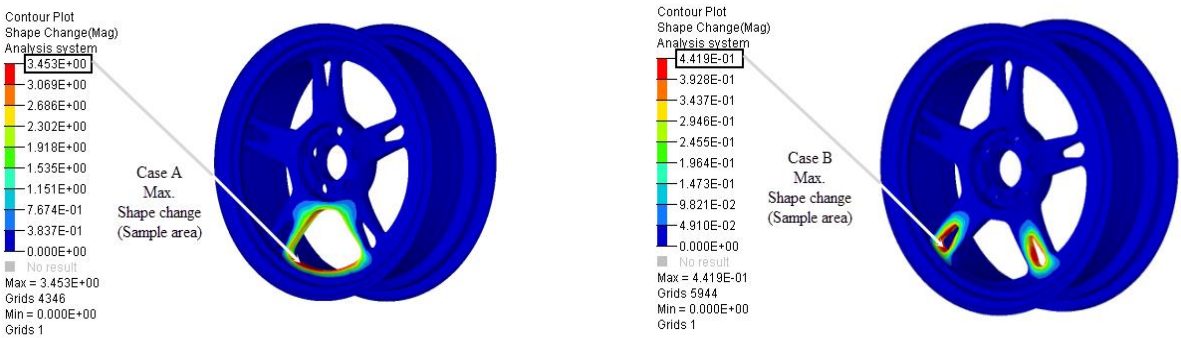
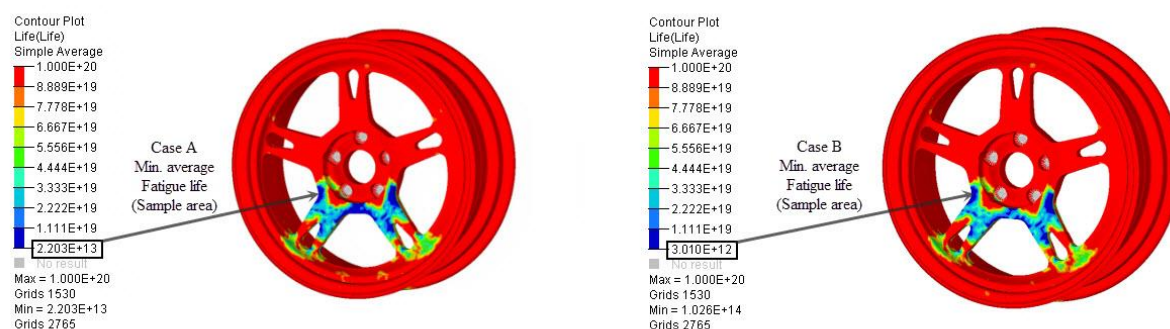**Figure 26:** Contour of shape changes, Case A and Case B

Figure 27: Contour of fatigue life, Case A and Case B

The contours of shape changes as a result of boundary nodes movements through the shape optimization process are presented in Figure 26. The fatigue life contours as a result of Free-shape optimization are presented in Figure 27.

5.4 Comparison of Shape Optimization, Case A and Case B

1) Referring to Table 10, considering the fatigue life enhancement criteria, it is clear that shape optimization Case A, is more effective than Case B.

2) Since, the automotive wheel has geometrical symmetry, regarding the dynamic and static balance of automotive wheel, the shape changes in the Case A can be extended to other wheel spokes.

6. Case Study

In this case study, the optimized wheel is compared to a wheel in the market (Figure 28) by static and fatigue analysis. The size (7.5 inches width and 18 inch diameter), material (Table 3) and the finite element model of both wheels are considered the same.

The maximum magnitude of normal, lateral and longitudinal loadings corresponding to the most severe test condition (Table 7) are considered in static analysis and the corresponding normalized load-time histories (Figures 17, 18 and 19) are allocated to mentioned static loadings and used in fatigue analysis. The results of fatigue analysis are shown in Figure 29. The fatigue analysis results show that optimized wheel has better fatigue behavior characteristics compared to the wheel in the market (Min. average fatigue life of $2.203*10^{13}$ for the optimized wheel against $1.039*10^{11}$ for the wheel in the market).

The contours of Von Mises stress as results of normal, lateral, longitudinal loadings and tire inflation pressure are shown in Figures 30, 31, 32 and 33, respectively.

By comparison of the maximum Von Mises stress in all types of considered loadings, the optimized wheel design shows acceptable strength characteristics. Therefore, the optimized wheel has acceptable fatigue and strength characteristics.

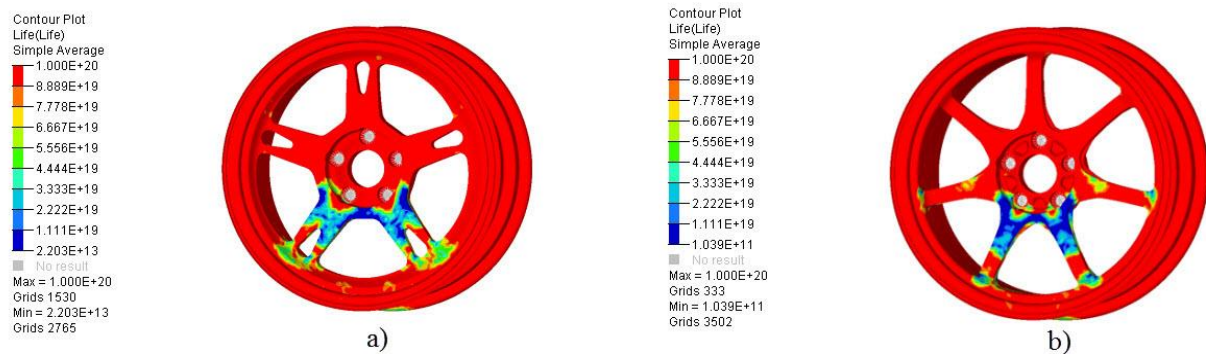**Figure 28:** a) Optimized Wheel, b) Wheel in the market

Figure 29: Contour of fatigue life a) Optimized Wheel A, b) Wheel in the market
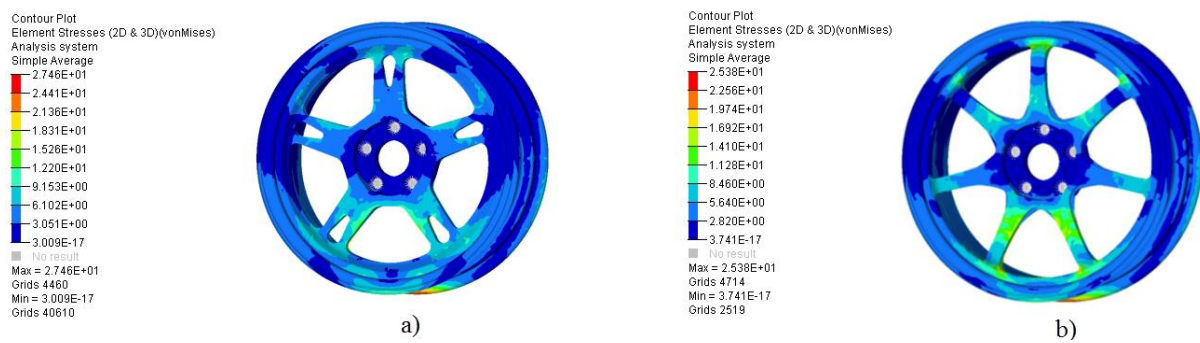

Figure 30: Von Mises stress of Normal loading, a) Optimized Wheel A, b) Wheel in the market
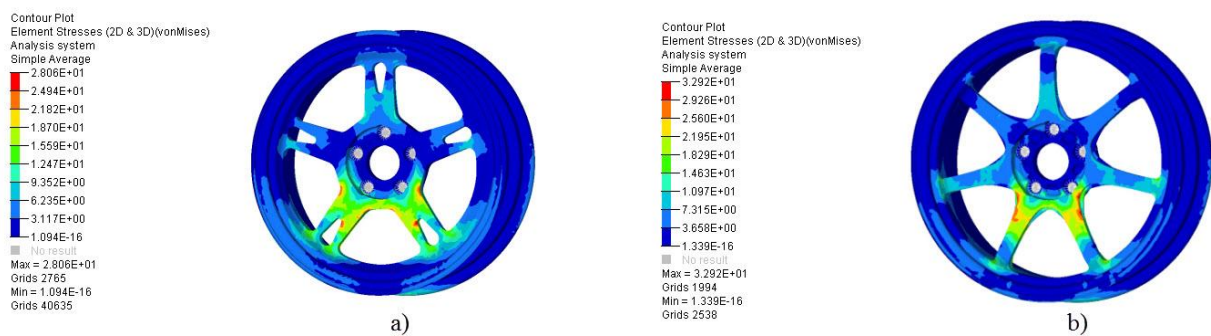

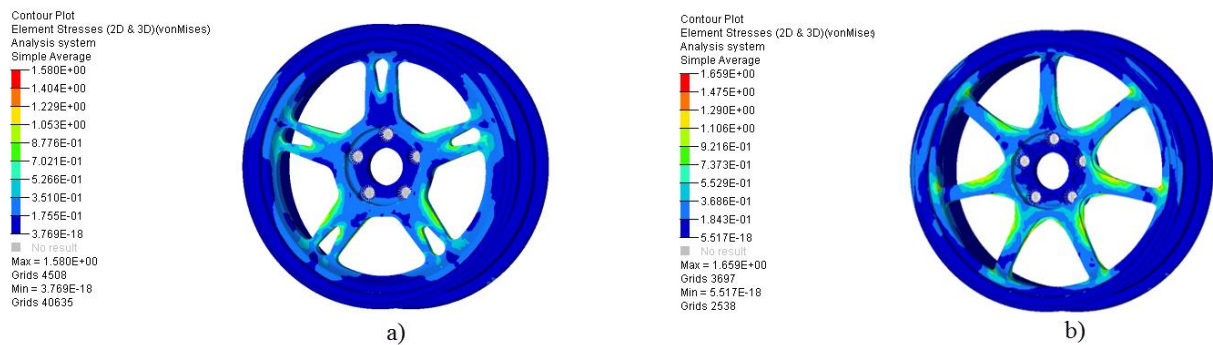**Figure 31:** Von Mises stress of Lateral loading, a) Optimized Wheel, b) Wheel in the market

Figure 32: Von Mises stress of Longitudinal loading, a) Optimized Wheel, b) Wheel in the market
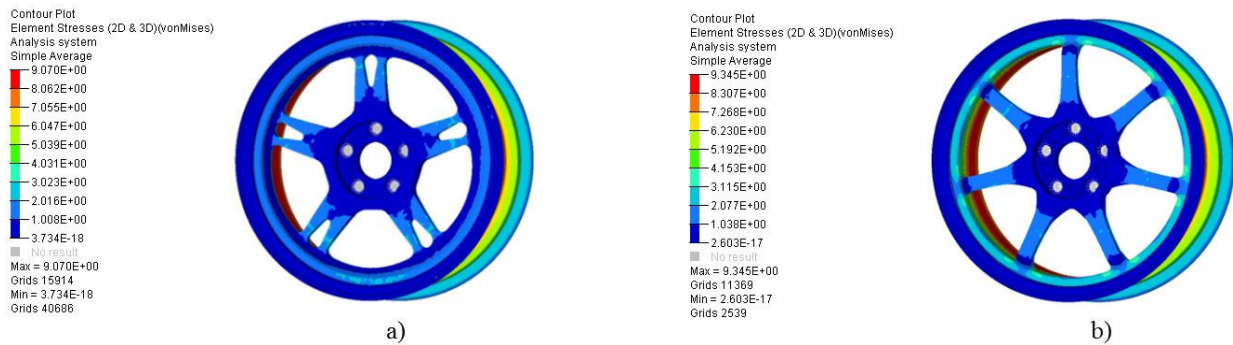
Figure 33: Von Mises stress of Tire Inflation pressure, a) Optimized Wheel A, b) Wheel in the market

7. Conclusions

In this study, a two-step optimization procedure is introduced. At first, topology optimization method is applied to a primary automotive wheel model followed in the next stage by shape optimization method. The results show 31.841% weight and 33.047% compliance reductions by topology optimization and also 652.33% average minimum fatigue life enhancement, by the shape optimization.

The results represent the ability of topology optimization in presenting a new lightweight design of the automotive wheel, regarding the design requirements (e.g. stiffness) and the ability of shape optimization in improving the initial design (e.g. fatigue life enhancement). The method used in this study can be extended to optimization of other automotive components.

References

[1] M. Grujicic, G. Arakere, P. Pisu, B. Ayalew, Norbert Seyr, Marc Erdmann, and Jochen Holzleitner. "Application of topology, size and shape optimization methods in polymer metal hybrid structural lightweight engineering." Multidiscipline Modeling in Materials and Structures 4, no. 4 (2008): 305-330.

[2] E. Pagnacco, S. Lambert, L. Khalij, and D. A. Rade. "Design optimisation of linear structures subjected to dynamic random loads with respect to fatigue life." International Journal of Fatigue 43 (2012): 168-177.

[3] P. Li, D. M. Maijer, T. C. Lindley, and P. D. Lee. "A through process model of the impact of in-service loading, residual stress, and microstructure on the final fatigue life of an A356 automotive wheel." Materials Science and Engineering: A 460 (2007): 20-30.

[4] M. Haiba, D. C. Barton, P. C. Brooks, and M. C. Levesley. "The development of an optimisation algorithm based on fatigue life. "International Journal of Fatigue 25, no. 4 (2003): 299-310.

[5] B. Desmorat, R. Desmorat. "Topology optimization in damage governed low cycle fatigue." Comptes Rendus Mecanique 336, no. 5 (2008): 448-453.

[6] M. Topac, M., S. Ercan, and N. S. Kuralay. "Fatigue life prediction of a heavy vehicle steel wheel under radial loads by using finite element analysis." Engineering Failure Analysis 20 (2012): 67-79.

[7] W. W. Muhamad, , E. Sujatmika, M. R. Idris, and SA Syed Ahmad. "An Optimization Analysis on an Automotive Component with Fatigue Constraint Using HyperWorks Software for Environmental Sustainability. "World Academy of Science, Engineering and Technology, International Journal of Mechanical, Aerospace, Industrial, Mechatronic and Manufacturing Engineering 6, no. 8 (2012): 1395-1399.

[8] E. Holmberg, B. Torstenfelt, A. Klarbring. Fatigue constrained topology optimization." Structural and Multidisciplinary Optimization 50.2 (2014): 207-219.

[9] S. H. Jeong, D.H. Choi, G. H. Yoon. "Fatigue and static failure considerations using a topology optimization method." Applied Mathematical Modelling 39.3-4 (2015): 1137-1162.

[10] M. Collet, M. Bruggi, P. Duysinx. "Topology optimization for minimum weight with compliance and simplified nominal stress constraints for fatigue resistance." Structural and Multidisciplinary Optimization 55.3 (2017): 839-855.

[11] J. Oest, E. Lund. "Topology optimization with finite-life fatigue constraints." Structural and Multidisciplinary Optimization 56.5 (2017): 1045-1059.

[12] N. Hägele, and C. M. Sonsino. "Structural durability design recommendations for forged automotive aluminium chassis components submitted to spectrum and environmental loadings by the example of a tension strut." International Journal of Fatigue 69 (2014): 63-70.

[13] J.Y.Wong, Theory of ground vehicles. John Wiley & Sons, New York (2001).

[14] D.A. Hullender, "Generation of a random time series with a specified spectral density

function," In Joint Automatic Control Conference, 16, (1979) :532-535.

[15] A. Tang, N. Tamini , D.Yang. "Virtual proving ground–a CAE tool for automotive durability, ride & handling and NVH applications." In 6th International LS-DYNA users conference, Detroit (2000).

[16] R.I. Stephens, A. Fatemi, R.R.Stephens, H.O. Fuchs. "Metal fatigue in engineering. John Wiley & Sons, New York (2000).

[17] M.P. Bendsøe, N. Kikuchi. "Generating optimal topologies in structural design using a homogenization method. "Computer methods in applied mechanics and engineering, 71, 2, (1988): 197-224.

[18] O.M. Querin, G.P. Steven, Y.M. Xie. "Evolutionary structural optimisation using an additive algorithm." Finite Elements in Analysis and Design, 34, 3, (2000): 291-308.

[19] G.I. Rozvany, "A critical review of established methods of structural topology optimization." Structural and Multidisciplinary Optimization, 37, 3, (2009): 217-237.

[20] J. Shen, D. Yoon. "A new scheme for efficient and direct shape optimization of complex structures represented by polygonal meshes." International journal for numerical methods in engineering, 58, 14, (2003): 2201-2223.

[21] D. Gao, D. Wang, G. Wang, L. Hao. "Topology optimization of conditioner suspension for mower conditioner considering multiple loads." Mathematical and Computer Modelling, 58, 3, (2013): 489-496.

[22] M. Bruyneel, P. Duysinx, C. Fleury. "A family of MMA approximations for structural optimization." Structural and Multidisciplinary Optimization, 24, 4, (2002): 263-276.

[23] K. Svanberg, "The method of moving asymptotes-a new method for structural optimization." International journal for numerical methods in engineering, 24, 2, (1987): 359-373.

[24] C. Fleury. "CONLIN: an efficient dual optimizer based on convex approximation concepts." Structural optimization, 1, 2, (1989): 81-89.

[25] C. Fleury. "Mathematical programming methods for constrained optimization" dual methods." Progress in astronautics and aeronautics, 150, (1993): 123-150.

[26] G. Zoutendijk. Methods of feasible directions: a study in linear and non-linear programming, Elsevier, Amsterdam (1960).

[27] D. Z. Du, W. Wu, P. M. Pardalos, N. Sohaee. "Feasible Direction Method." Wiley Encyclopedia of Operations Research and Management Science (2012